Numerical Simulation of South China Sea Wave under Typhoon and Winter Monsoon Effects

Kuo-Feng CHENG
Numerical Forecast Center
Chinese Naval Meteorologic and Oceanographic Office

ABSTRACT

Oceanic wave responses to tropical cyclones have been well identified in the Hurricane Region (i.e. Western Atlantic Ocean), but not in the Typhoon Region (the Western Pacific Ocean), especially in the regional seas as South China Sea. Essentially, this is due to lack of observational and modeling studies in this region. To fill this gap, Wavewatch-III (WW3) is used to study the response of the South China Sea (SCS) to Typhoon Muifa (2004). The major purposes are to find the similarity and dissimilarity of wave characteristics between the two regions, and to evaluate the WW3 capability under typhoon forcing. The WW3 model is integrated from the JONSWAP wave spectra with a calculated sea surface wind dataset of Typhoon Muifa, from 16 November to 25 November 2004. The 2-dimension spectral analysis is applied to examine the wave characteristics of SCS under typhoon forcing, as well as the effects of winter monsoon and topography. This study shows strong similarities in the wave responses between HR and TR, including strong energy in the right-front quadrant of the typhoon center, and asymmetry in the directional wave spectra at different locations (frontward, backward, rightward, and leftward) around the typhoon center. Some unique features of the SCS wave characteristics to Muifa are also discussed.

Key word: WAVEWATCH-III, sea surface wave, numerical simulation, South China Sea, Typhoon Muifa (2004)

I. Introduction

A hurricane with intense and fast-varying wind produces a severe and complex ocean wave field that can propagate for thousands of kilometers away from the storm center, resulting in dramatic variation of the wave field in space and time (Barber and Ursell 1948). Various instruments have been applied to measure and investigate the hurricane-generated wave and its characteristics in wave height, directional wave spectra, and wave propagation (Holt et al. 1998; Wright et al. 2001; Walsh et al. 2002). A Atlantic Ocean hurricane observation (Wright et al. 2001) show that the significant wave height (H_s) reaches 14 m in the open ocean; the maximum wave heights appear in the right forward quadrant of the hurricane center and propagate in the same direction as the hurricane. Moon et al. (2003) simulated the wave characteristics for the same hurricane successfully using the wave model WAVEWATCH-III (WW3) and found that the hurricane-generated wave field is mostly determined by two factors: the distance from the hurricane center or radius of maximum wind and hurricane translation speed (HTS). But for the low HTS case, the dominant wave direction is mainly determined by the distance and direction from the hurricane center. The directional wave spectra around the hurricane center in a maximum wind radius (R_m) show that the wave spectra in the east and the north locations have a unilateral shape due to resonance effect, and the spectra in the west and the south locations have a more complex structure.

Previous studies mostly identified the oceanic wave in open oceans and in the Western Atlantic Ocean (Hurricane Region, HR). Few observational and/or modeling studies have been done in the Typhoon Region (TR), especially in the South China Sea (SCS). The SCS is one of the largest marginal seas of the Western Pacific Ocean, extending across tropical and subtropical zones and encompasses a total surface area of 3.5×10^6 km^2 (Figure 1). Due to its semi-enclosed nature, the SCS is subject to high spatial and temporal variability from external forcing factors. Also a significant source of the SCS variability is the tropical cyclones that routinely affect the region. Our goal in this study is to identify if those effects occurring in HR still exist in TR.

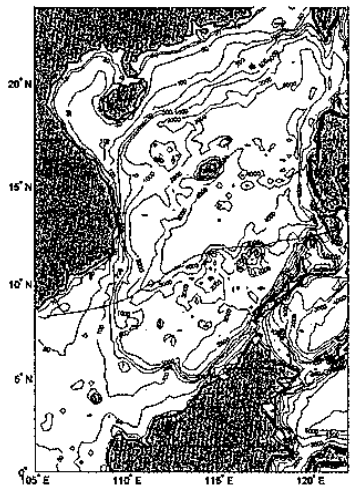

Figure 1 The SCS bathymetry. Red line indicate TY Muifa track.

II. Typhoon Muifa (2004)

Typhoon (TY) Muifa is one of the four tropical cyclones passing by the SCS in 2004. It was formed on 11 November and weakened over land on 26 November (JTWC 2005). The best track record of TY Muifa is shown as Table 1 and red line in Figure 1. Since the SCS in-situ wind observations were difficult to conduce during typhoon seasons, the QuikSCAT (QSCAT) remotely sensed data may provide surface wind. However, strong rotational motions of TY Muifa were not represented in the QSCAT data due to the spatial coverage(Figure 2a). To overcome this deficiency, a Tropical Cyclone Wind Profile Model (TCWPM) (Carr and Elsberry 1997) is used to produce the high resolution surface wind for TY Muifa. The procedure is: first, the temporally average of QSCAT data is taken from ascending and descending passes during 16-25 November as the background wind, which also represents the dominant winter monsoon in the SCS; then the total wind field is computed using TCWPM from 0000UTC 16 November to 0600UTC 25 November for (0°-25°*N*, 105°-122°*E*) on a 1/4°×1/4° grid with the time interval of 6 hr. Such a wind field is referred to "the QTCWPM wind" (Figure 2b).

The daily evolution of the QTCWPM winds (Figure 2a) shows that the wind speed increases as TY Muifa enters the SCS, and decreases as Muifa approaches the land. The maximum speed of QTCWPM wind is comparable to the maximum wind speed reported in the best track record (46.3 m/s). The QTCWPM wind is compared to the QSCAT wind as well as to the National Centers for Environmental Prediction (NCEP) surface winds grid. The root mean square error (RMSE) is 3.2 m/s between QTCWPM and NCEP winds and 3.4 m/s between QTCWPM and QSCAT winds. Furthermore, a set of ideal typhoon wind (Figure 2c) is generated with zero background winds in order to separate and compare typhoon and monsoon forcing for the ocean waves. As mentioned above, the SCS background wind field during TY Muifa is considered as the winter monsoon. The maximum wind speed is about 46.3 m/sec. Before arrival and after departure of TY Muifa, the wind speed is closed to zero. Besides, the wind speed is also zero far from the typhoon track. This wind field is referred to "the ideal typhoon wind" to examine the monsoon effect in the following simulation.

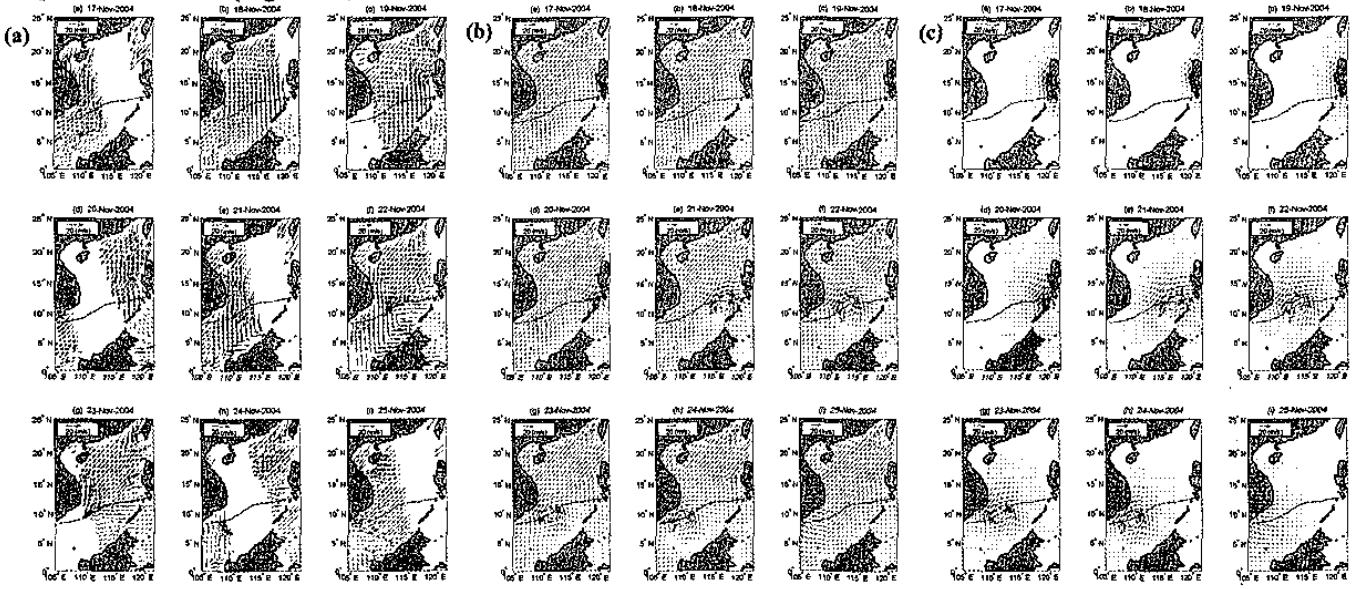

Figure 2 Daily evolution of different wind fields on 17-25 November 2004.
(a) QSCAT satellite observed wind. (b) QTCWPM wind. (c) Ideal typhoon wind.

Figure 3

Date/Time	Lat (N)	Long (E)	Pressure (μPa)	V_{max} (m/sec)	Date/Time	Lat (N)	Long (E)	Pressure (μPa)	V_{max} (m/sec)
11/16/2004 00:00	14.5	125.7	994	20.6	11/20/2004 12:00	12.3	119.3	980	30.9
11/16/2004 06:00	14.5	124.9	991	23.1	11/20/2004 18:00	12.2	118.3	976	33.4
11/16/2004 12:00	14.5	124.2	984	28.3	11/21/2004 00:00	11.9	117.2	976	33.4
11/16/2004 18:00	14.4	123.6	984	28.3	11/21/2004 06:00	11.9	116.1	972	36
11/17/2004 00:00	14.6	123.6	980	30.9	11/21/2004 12:00	11.8	115.2	963	41.2
11/17/2004 06:00	14.8	123.6	976	33.4	11/21/2004 18:00	11.6	114.4	954	46.3
11/17/2004 12:00	15.2	123.8	967	38.6	11/22/2004 00:00	11.4	113.6	958	43.7
11/17/2004 18:00	15.5	123.8	954	46.3	11/22/2004 06:00	11.1	113.1	958	43.7
11/18/2004 00:00	15.7	123.8	938	54	11/22/2004 12:00	10.8	112.6	967	38.6
11/18/2004 06:00	15.9	123.9	927	59.2	11/22/2004 18:00	10.5	112.1	976	33.4
11/18/2004 12:00	15.9	124.2	927	59.2	11/23/2004 00:00	10.1	111.7	976	33.4

11/18/2004 18:00	15.7	124.4	938	54	11/23/2004 06:00	9.9	111.1	976	33.4
11/19/2004 00:00	15.2	124.2	938	54	11/23/2004 12:00	9.6	110.6	980	30.9
11/19/2004 06:00	14.7	124.1	954	46.3	11/23/2004 18:00	9.3	110.2	984	28.3
11/19/2004 12:00	14.2	123.7	958	43.7	11/24/2004 00:00	9.1	109.7	984	28.3
11/19/2004 18:00	13.7	122.8	963	41.2	11/24/2004 06:00	8.8	108.8	987	25.7
11/20/2004 00:00	12.8	121.6	967	38.6	11/24/2004 12:00	8.5	107.4	994	20.6
11/20/2004 06:00	12.5	120.3	976	33.4	11/24/2004 18:00	8.3	105.7	994	20.6
11/20/2004 12:00	12.3	119.3	980	30.9	11/25/2004 00:00	8.7	103.6	994	20.6

Table 1 The best track record of TY Muifa (2004) from 0000UTC 16 November to 0600UTC 25 November (from JTWC 2005).

III. WW3 Evaluation during TY Muifa

WW3 is a fully spectral third-generation ocean wind-wave model (Tolman1999). It has been validated over global and regional scale wave forecasts (Wittmann 2001; Tolman et al. 2002). The WW3 capability for the SCS wave simulation has also been verified using the TOPEX/Poseidon (T/P) and European Remote Sensing Satellites (ERS-1/2) data (Chu et al. 2004). For the evaluation during TY Muifa, this study uses a relatively high resolution setting for the WW3 model (Wittmann 2001; Tolman et al. 2002). The spatial resolution is 1/4°×1/4° in the SCS of latitude 0°-25°*N*, and longitude 105°-122°*E*. The discretization of energy spectra is in 24 directions (15° spacing), and in 25 frequencies with logarithmic increment from 0.0418 to 0.3058 Hz. Two time step values are used for computational efficiency. The global time step, the spatial time step, and the spectral time step are all set to 300 second, for entire solution propagation, spatial propagation, and intra-spectral propagation, respectively. The source time step for the source term integration is set to 100 second. The QUICKEST with ULTIMATE propagation scheme is used here. The source components are using Tolman and Chalikov (1996) wind-wave interaction and dissipation terms, the DIA nonlinear interaction term, and the JONSWAP bottom friction term, respectively.

The QTCWPM wind is used as input to drive WW3 for the SCS. WW3 is run from 0000UTC 16 November to 1200UTC 25 November. Since TY Muifa entered the SCS as late as 19 November, the model computation of the first three days, from 16 to 18 November, could be considered as the 'spin up' period of WW3 model. During the duration of TY Muifa (2004), the temporal covered cycles of T/P are 448, which from 11 to 21 November, and 449, from 21 November and 01 December. There are 14 passes across the SCS area, which include 001, 012, 038, 051, 064, 077, 088, 114, 127, 140, 153, 164, 216, and 229. These passes have total 25 crossover points in the ocean region. On each point, the significant wave height (H_s) from T/P measurement is accumulated to evaluate the H_s from WW3 computation.

The comparison between WW3 result and T/P observation is computed and performed as Figure 4. The total number of H_s pairs during the duration of TY Muifa is 38. The scattering diagram (Figure 4a) shows the clustering of points approximately located around the equal line. The histogram of the differences between model and observation (Figure 4b) shows a Gaussian-type distribution. Examining the statistics, the bias of two datasets is 0.137 m with RMSE is 0.308 m, and the correlation coefficient is 0.895. The statistics suggests that the WW3 result and the T/P observation agreed well, and the numerical simulation during the duration of TY Muifa is accurate and reasonable.

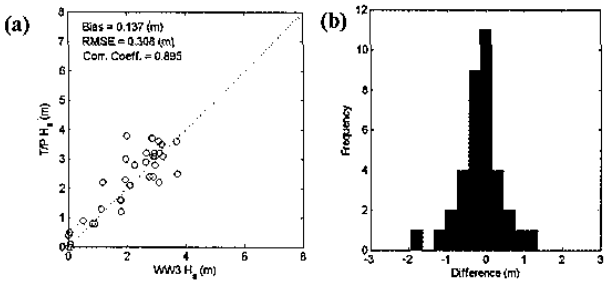

Figure 4 The comparison of WW3 result and T/P observations on all crossover points in the duration of TY Muifa (2004). (a) The paired data distribution; and (b) the histogram distribution of difference.

IV. SCS Wave Simulation

1. Numerical simulation Scheme

The numerical simulations of the SCS wave were analyzed with three scenarios. (1) Realistic wind and bottom topography: the QTCWPM wind with the 1/12°×1/12° resolution global bathymetry dataset. (2) Ideal typhoon wind and realistic bottom topography: the "ideal typhoon wind" with the same global bathymetry dataset. (3) Ideal typhoon wind and uniform bottom topography: the "ideal typhoon wind" with the remove of surrounding islands (Taiwan, the Philippians Islands, Palawan, Borneo, and the Indonesia Islands) and a uniform depth of 2000 m. The daily evolution of H_s in the SCS during TY Muifa is exhibited for comparisons between three scenarios. The typhoon effect was simulated using the ideal typhoon wind (Scenario-2). The monsoon effect was simulated using the difference between Scenario-1 and Scenario-2. Use of the uniform bottom topography represented the open ocean case. The topographic effect was examined by the difference between Scenario-2 and Scnario-3.

2. Spectral Analysis at Typhoon Intense Center

The location of extreme situation of TY Muifa was selected to conduce the directional wave spectra and to investigate the distance and direction from typhoon center, and the typhoon intensity. At 1800UTC 21 November, TY Muifa reached the strongest intensity (i.e.,

the lowest central pressure, 954μPa) at the location, (11.6°N, 114.4°E). The maximum wind speed was 46.3 m/s, and Rm was 14.0 km. At that time, the HTS slowed down to 4.2 m/s. This location is referred as the "typhoon intense center". Four-way locations are designed around the typhoon intense center with the R_m away to investigate the effect of location and direction for the typhoon center on the directional wave spectra,: forward location (F), backward location (B), rightward location (R), leftward location (L), and the typhoon intense center (C) (see up-left panel of Figure 5).

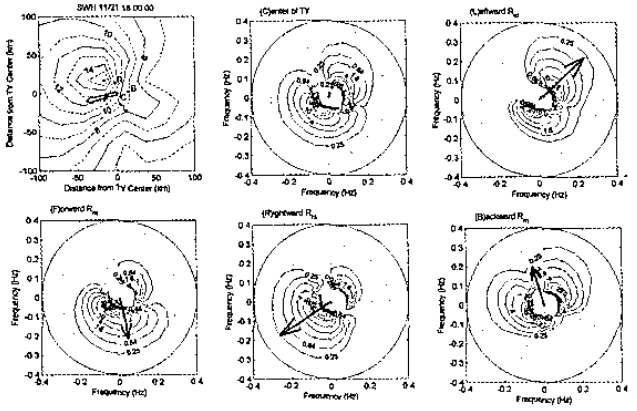

Figure 5 H_s, and central (C) and four-way (F, R, L, and B) directional wave spectra of the typhoon intense center (1800UTC 21 November, 11.6°*N*, 114.4°*E*). The hollow arrow is the translation direction.

V. Typhoon Wind Effects

1. Significant Wave Height

Figure 6 shows the daily H_s in the SCS during TY Muifa. The color scale symbolizes the value of H_s, from blue (0 m) to red (16 m). Here, the upper panels (Figure 6a-c) are for the period of TY Muifa entering the SCS; the middle panels (Figure 6d-f) are for the period of TY Muifa passing the SCS; and the lower panels (Figure 6g-i) shows the period of TY Muifa leaving the SCS. Comparing to the evolution of QTCWPM wind (Figure 2b), it is found that the distribution of H_s follows the moving TY Muifa. High H_s is with high wind speed and high waves appear to the right of the typhoon track. The maximum H_s (16 m) presents as TY Muifa reaches the intense center. Another high H_s occurs in east of Luzon on 24 and 25 November (Figure 6h-i). It is shown that the difference in monsoon-generated waves before TY Muifa arrival (Figure 6a-c) and after TY Muifa departure (Figure 6g-i). This indicates that the existing typhoon-generated wave field may affect the generation of new wind-wave field.

While reviewed Figure 2b, the core of the maximum wind speed is almost symmetric along TY Muifa track. However, the core of the maximum Hs is asymmetric in width and in value along the track of TY Muifa (Figure 6) with higher Hs in the right side of the track than the left side. At the typhoon intense center, Figure 5a shows the horizontal distribution of Hs with the THS direction (in hollow arrow) of Muifa. Rm is 14.0 km (in dashed circle). Along the HTS direction, the high values of Hs are in the right forward quadrant with the maximum Hs of 16 m slightly outside of Rm from the typhoon center. This consists with earlier studies (Moon et al. 2003) that the wave generation on the typhoon center has an asymmetric distribution in four quadrants.

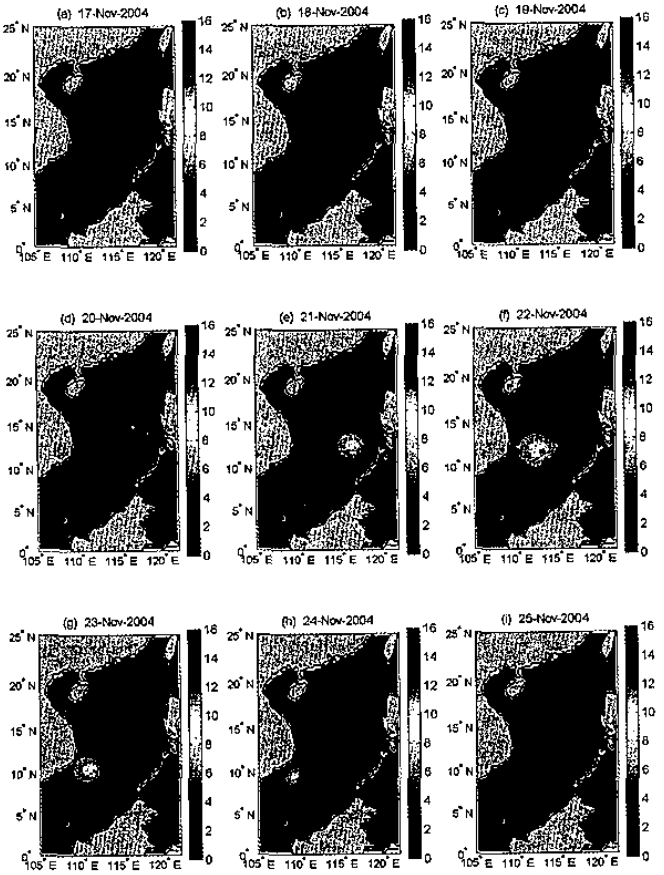

Figure 6 Daily SCS wave evolution during TY Muifa (2004).

2. Directional Wave Spectra at Intense Center

Figure 5 shows the analysis of four-way locations around the typhoon intense center. The dashed circle shows TY Muifa R_m. The hollow arrow indicates the typhoon translation vector and the solid arrow is the wind vector. The waves are generated in both frontward and backward directions for the typhoon intense center (Figure 5C). The directional wave spectra are very different at locations (F, R, and L). Two wave packets are generated in both upwind and downwind directions at locations (F, R, and L). It shows the consistence with the previous study (Moon et al. 2003) that high-frequency waves are generated aligning the wind direction due to resonant effects in the forward and rightward directions. But in the leftward and backward directions, the wave spectra have a complicated structure. Figure 7 shows the daily directional wave spectra at the typhoon intense center. The solid arrow indicates the wind vector. The winds (7.8 m/s) blow from northeast (45° from the north) before 1800UTC 20 November and after 1800UTC 23 November, showing the winter monsoon dominates. In these two periods, a set of low-frequency waves exists and aligns with the wind in a slight angle leftward. Conversely, from 1800UTC 20 November to 1800UTC 23 November, rapid change of waves in both direction and frequency is found. Furthermore, after the departure of TY Muifa, evident wave packet still remains in the direction from 30° to 70°.

This shows the wave energy remains for two days after TY Muifa departure, and then disperses.

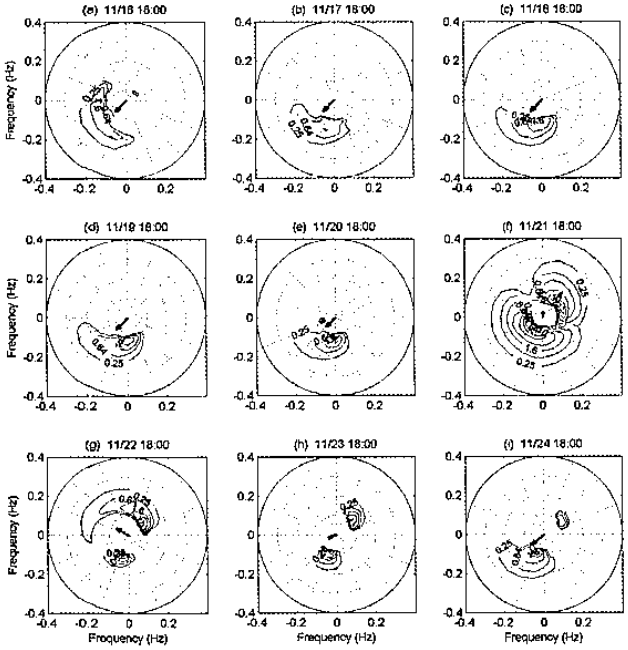

Figure 7 Daily directional wave spectra at the typhoon intense center with QTCWPM wind. The time step is 24 hours. The arrow presents QTCWPM wind vector. The wind speed is 100 times of the axis scale.

VI. Other Effects

1. *Effects of Monsoon Winds*

The ideal typhoon wind (Figure 2c) is used as the wind input for WW3 to separate the effect of winter monsoon. The daily H_s in the SCS has also been produced but not shown here. It is found that the horizontal distribution of H_s is quite similar between the simulations of the ideal typhoon wind and the QTCWPM wind near TY Muifa track. But the maximum H_s using the ideal typhoon wind is 15 m and less than that using QTCWPM wind (16 m). Figure 10a shows mean differences of Hs field between the two simulations. The color scale is from -0.5 m (blue) to 2.5 m (red). The monsoon wind does not affect H_s near the typhoon track, but does affect H_s far from the typhoon track, especially in the northern SCS. The maximum H_s difference is located in the deep water area away from the coast. It indicates a fetch-limited case, which the higher waves produced farther from the coast by steady monsoon.

Figure 8 shows the daily evolution of directional wave spectra at the typhoon intense center. Compared Figure 7 with Figure 8, it is seen that the two directional wave spectra are almost the same at 1800UTC 21 November while TY Muifa passing to the point, but quite different for other time periods. Before TY Muifa arriving the intense center , there is high wave energy in the southwestward direction using the QTCWPM winds (Figure 7a-e) but none using the ideal typhoon wind (Figure 8a-e). After TY Muifa departure, the typhoon-generated waves in swell direction dispersed, and the swell energy appeared again (Figure 7g-i). Distinction between two wave spectra is the swell generation (no swell generation) in the southwestward direction with QTCWPM (ideal typhoon) winds. This difference is due to the background wind monsoon wind.

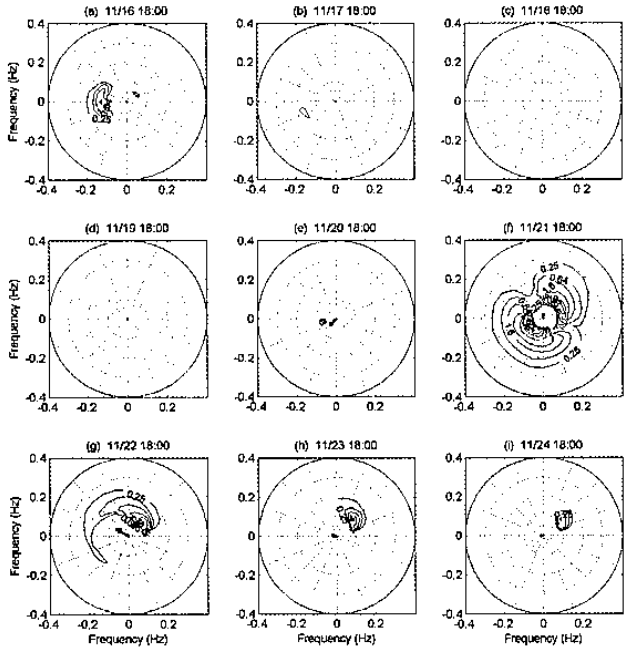

Figure 8 Similar format as Figure 7 at the typhoon intense center with ideal typhoon wind.

2. *Effects of Topography*

The third WW3 simulation is conducted by the ideal typhoon wind and uniform bottom topography to study the effects of island obstruction and bottom topography. Figure 9 shows this simulated daily H_s. The maximum H_s is about 15.5 m, which between using the realistic topography (15 m) and using the QTCWPM wind (16 m). As TY Muifa enters the SCS on 20 November, the typhoon-generated waves are well-developed due to no island obstruction. Although there is no island blockage in the left-rearward direction, the wave propagations are still limited. It is evident that along TY Muifa track, the typhoon generated waves more like to propagate in the right-backward and left-forward directions, and the right-forward and left-backward directions are restricted. It is also clear that the wave propagate faster than the typhoon translation. This may be due to the momentum flux into the typhoon passage in the right-forward and left-backward quadrants.

Figure 10 shows the mean H_s difference between realistic and uniform topography. It has similar figure setting as Figure 10, but the color scale smaller from 0 m (blue) to 1.5 m (red). The H_s using the uniform topography is developed better than using the realistic SCS topography, and the maximum difference is within 1.5 m. Large difference is seen along TY Muifa track while close to coastline. As TY Muifa close to the Asian landmass, the wave energy does not disperse due to no change in topography, and disappear only when the waves contact coastline.

The notable difference is also seen in the Gulf of Thailand, around Palawan, and in the west water of Borneo. In the east water of Borneo, previous simulation suggests that no wave propagation into it, but in this uniform topography simulation, the wave

propagation is observed. It shows that the SCS wave does not propagate into the Sulu Sea due to the obstruction of Palawan and Borneo. Therefore, the Sulu Sea may be considered as a different wave system from the SCS, and the wave simulation of the Sulu Sea in this study may be underestimated. Compared the difference in the south-west SCS with the bathymetry contour of the SCS (Figure 1),the difference of 0.5 m does follow 100 m water depth properly. This indicates that the topographic effect on the wave characteristics is not important when the local typhoon winds dominates with the water depth deeper than 100 m.

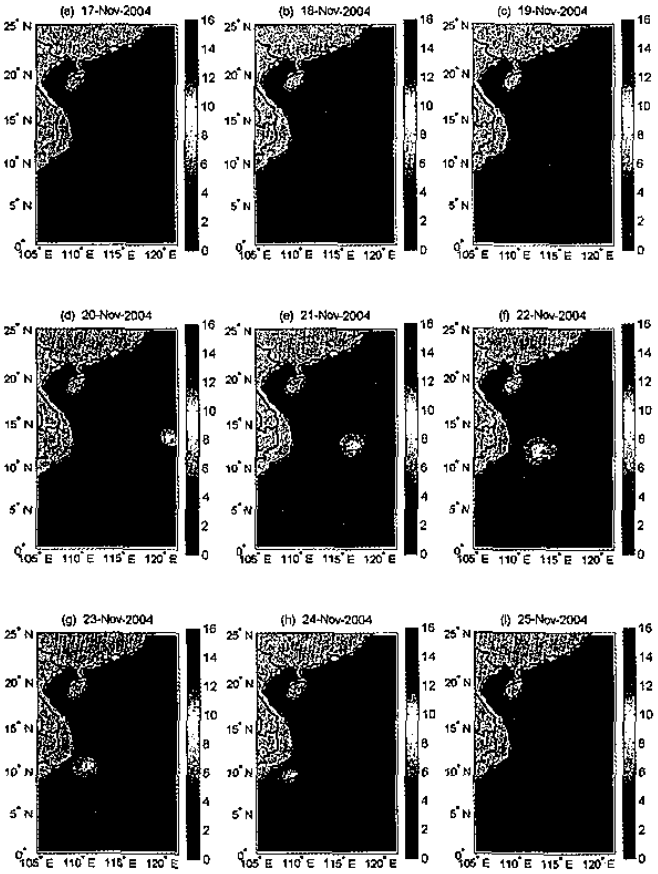

Figure 9 Daily SCS wave evolution with ideal typhoon wind and *uniform topography during* TY Muifa (2004)

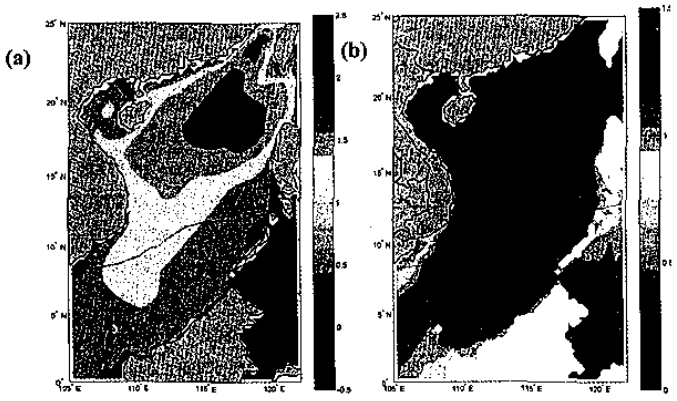

Figure 10 The mean H_s difference (a) between QTCWPM and ideal wind simulations (b) between realistic and uniform depth simulations.

VII. Conclusion

This study studied the SCS wave under typhoon and winter monsoon forcing using WW3. The WW3 model was forced by high resolution wind from the combination of QSCAT and TCWPM. The wave model was evaluated using the T/P altimetry observation during TY Muifa. Three scenarios were designed to analyze the effects of typhoon and monsoon on the SCS wave, and to compare it to the HR. The directional wave spectra near the typhoon intense center were produced to analyze the wave energy propagation and evolution.

Along typhoon translation track, the core of the maximum H_s was asymmetric with higher and wider core in the right side than the left side. The maximum H_s reached 16 m at the typhoon intense center. At a single point, the maximum H_s was always in the right-front quadrant of the typhoon center and located slightly outside the R_m. Before typhoon arrival, the monsoon-generated swell dominated and maximum H_s was about 4 m; after typhoon departure, the monsoon swell remained dominant and the typhoon-introduced wave decayed gradually and lasted for three days. The typhoon-generated wave propagated across the SCS to farther than 1000 km in only forward, left-frontward, and right-rearward directions of typhoon center.

Generally, the simulated wave characteristics in the TR are similar as those in the TR. The directional wave spectra were very different at the frontward, rightward, and leftward locations. At a single location, two wave packets were generated in both upwind and downwind directions as typhoon moving into the location. Low-frequency swell was generated by monsoon forcing; when the typhoon was present, the typhoon-introduced waves dominated and were much greater than monsoon-generated swell. The obstructions of coastline and small islands generated wave shadow zones along the wave propagation direction. It implies that the semi-closed SCS can be considered as an independent wave system from nearby oceans except the energy through the Luzon Strait. The Sulu Sea, which separated by the Palawan Island, can be seen as a different wave system from the SCS. The bathymetric effect was important only for water depth shallower than 100 m. For depth deeper than 100 m, the bathymetry may have an effect on H_s, but almost no effect on the wave propagation direction and decay frequency. Hence the intensity of typhoon, the distance and direction from typhoon center are more important factors than the monsoon, or the topography for the SCS wave.

The field observation in tropical cyclones of Powell et al. (2003) reports that the drag coefficient (C_d) is much less than previously thought in extreme high wind speed, i.e., above 40 m/s. At high wind speed, the overestimate of C_d in WW3 has also been reported (Moon et al. 2004). In the future, possible improvements may include a new scheme to compute the drag coefficient, and high resolution field wave observation in the TR.

References

Barber, N. F., and F. Ursell, 1948: "The generation and propagation of ocean waves and swell. I. Wave periods and velocities", Philosophical Transactions

of the Royal Society of London. Series A. Mathematical and Physical Sciences 240, 527-560.

Carr, L. E., III, and R. L. Elsberry, 1997: "Models of tropical cyclone wind distribution and beta-effect propagation for application to tropical cyclone track forecasting", Mon. Weather Rev. 125, 3190-3209.

Chu, P. C., Y. Q. Qi, Y. C. Chen, P. Shi, and Q. W. Mao, 2004: "South China Sea wind-wave characteristics. Part I: Validation of Wavewatch-III using TOPEX/Poseidon data", J. Atmos. Ocean. Technol. 21, 1718-1733.

Holt, B., A. K. Liu, D. W. Wang, A. Gnanadesikan, and H. S. Chen, 1998: "Tracking storm-generated waves in the northeast Pacific Ocean with ERS-1 synthetic aperture radar imagery and buoys", J. Geophys. Res. 103C, 7917-7929.

JTWC, cited 2006: 2004 annual tropical cyclone report. [http://www.npmoc.navy.mil/jtwc/atcr/2004atcr/].

Moon, I., I. Ginis, T. Hara, H. L. Tolman, C. W. Wright, and E. J. Walsh, 2003: "Numerical simulation of sea surface directional wave spectra under hurricane wind forcing", J. Phys. Oceanogr. 33, 1680-1706.

____, ____, and ____, 2004: "Effect of surface waves on air-sea momentum exchange. Part II: Behavior of drag coefficient under tropical cyclones", J. Atmos. Sci. 61, 2334-2348.

Powell, M. D., P. J. Vickery, and T. A. Reinhold, 2003: "Reduced drag coefficient for high wind speeds in tropical cyclones", Nature 422, 279-283.

Tolman, H. L., 1999: User Manual and System Documentation of WAVEWATCH-III version 1.18, NOAA/NCEP Tech. Note 166, 110 pp.

____, B. Balasubramaniyan, L. D. Burroughs, D. V. Chalikov, Y. Y. Chao, H. S. Chen, and V. M. Gerald, 2002: "Development and implementation of wind-generated ocean surface wave models at NCEP", Wea. Forecast 17, 311-333.

____, and D. Chalikov, 1996: "Source terms in a third-generation wind wave model", J. Phys. Oceanogr. 26, 2497-2518.

Walsh, E. J., D. W. Hancock III, D. E. Hines, R. N. Swift, and J. F. Scott, 1989: "An observation of the directional wave spectrum evolution from shoreline to fully developed", J. Phys. Oceanogr. 19, 670-690.

Wittmann, P. A., 2001: "Implementation of WAVEWATCH III at Fleet Numerical Meteorology and Oceanography Center", Oceans 3, 1474-1479.

Wright, C. W., E. J. Walsh, D. Vandemark, W. B. Krabill, A. W. Garcia, S. H. Houston, M. D. Powell, P. G. Black, and F. D. Marks, 2001: "Hurricane directional wave spectrum spatial variation in the open ocean". J. Phys. Oceanogr. 31, 2472-2488.